JOURNAL OF THERMOPHYSICS AND HEAT TRANSFER
Vol. 17, No. 3, July–September 2003

# Heat-Transfer Coefficients of a Turbine Blade-Tip and Near-Tip Regions

Jae Su Kwak* and Je-Chin Han†
*Texas A&M University, College Station, Texas 77843-3123*

**The detailed distribution of heat-transfer coefficients on a gas turbine blade tip was measured using a hue-detection-based transient liquid crystals technique. The heat-transfer coefficients on the shroud and near-tip regions of the pressure and suction sides of a blade were also measured. Tests were performed on a five-bladed linear cascade with a blowdown facility. The Reynolds number based on the cascade exit velocity and axial chord length of a blade was $1.1 \times 10^6$, and the overall pressure ratio was 1.2. The heat-transfer measurements were made at the three different tip gap clearances of 1.0, 1.5, and 2.5% of blade span. Results showed that, in general, the heat-transfer coefficients on the tip surface were higher than these on the shroud and on the near-tip region of the blade pressure and suction sides. Results also showed that as the tip gap clearance increased the heat-transfer coefficients increased on the tip surface, but the shroud and the blade suction side increased and then decreased. However, the heat-transfer coefficients on the blade pressure side remained almost unchanged as the tip gap clearance increased.**

## Nomenclature

| | | |
|---|---|---|
| $C$ | = | tip clearance gap, % of the blade span or mm |
| $C_x$ | = | axial chord length of the blade, 8.61 cm |
| $h$ | = | local convective heat-transfer coefficient, W/m$^2$K |
| $\bar{h}$ | = | averaged heat-transfer coefficient at a given $x/C_x$, W/m$^2$K |
| $k$ | = | thermal conductivity of blade-tip material, 0.18 W/m K |
| $P$ | = | local static pressure, kPa |
| $P_t$ | = | total pressure at the cascade inlet, kPa |
| $T_i$ | = | initial temperature of the blade-tip surface, °C |
| $T_m$ | = | temperature of the mainstream at the cascade inlet (recovery temperature), °C |
| $T_w$ | = | color change temperature of the liquid crystals, °C |
| $Tu$ | = | turbulence intensity level at the cascade inlet, % |
| $t$ | = | transition time for liquid crystals color change, s |
| $x$ | = | axial distance, cm |
| $\alpha$ | = | thermal diffusivity of blade tip material, $1.25 \times 10^{-7}$ m$^2$/s |
| $\tau_i$ | = | step change of time, s |

## Introduction

THE continuing trend toward high gas-turbine inlet temperature has resulted in a high heat load on turbine components. Blade tips are one of the regions susceptible to failure caused by the large thermal load and difficulty in cooling. For the typical gas-turbine rotor blade there is a gap between the rotating blade tip and the stationary shroud surface called the tip gap clearance. Blade-tip failure is caused primarily by hot gas flow through the tip gap. Hot gas leaks through the tip gap clearance because of pressure differences between the blade pressure and the suction side, causing a thin boundary layer and a high heat-transfer coefficient. Thus, it is important to investigate the heat-transfer coefficient distribution on blade-tip and near-tip regions.

Recently, many researchers have paid attention to turbine blade-tip heat transfer. Mayle and Metzger[1] studied heat transfer in a two-dimensional rectangular tip model with and without rotating shroud. They noted that the effect of blade rotation could be neglected to access the blade-tip heat transfer over the entire range of parameters considered in the study. Metzger and Rued[2] presented heat-transfer and flow results in the near-tip region of the pressure surface using a blade-tip simulation and sink flow. Their model simulated a sink flow similar to the sink-like characteristics of the blade tip gap on the pressure side. Rued and Metzger[3] presented heat-transfer and flow results in the near-tip region of the suction surface using a blade-tip simulation and a source flow. Their model simulated a blade suction surface with a gap feeding a source flow similar to the flow exiting the tip gap on the suction surface of an airfoil.

Metzger et al.[4] and Chyu et al.[5] studied heat transfer for both flat and grooved rectangular tip models. They confirmed that relative motion had little effect on the averaged heat transfer on the tip, although some local effects were observed.

There are very limited data in the open literature on blade-tip heat transfer in a cascade environment. Metzger et al.[6] used heat-flux sensors to measure local heat flux in a rotating turbine rig with two different tip gaps. Bunker et al.[7] investigated the detailed distribution of heat-transfer coefficients on the blade-tip surface using a hue-detection-based liquid crystals technique. They measured the heat-transfer coefficient at three tip gaps and two freestream turbulence levels with both sharp and rounded edges. Azad et al.[8,9] studied the flow and heat transfer on the first stage blade tip of an aircraft engine turbine (GE-E$^3$). They presented the effects of tip gap clearance and freestream turbulence intensity level on the detailed heat-transfer coefficient distribution for both plane and squealer tips under engine representative flow conditions. They used transient liquid crystals technique and found that the overall heat-transfer coefficients on the squealer tip were lower than those of the plane tip. Teng et al.[10] measured heat-transfer coefficients and static-pressure distriutions on a turbine blade tip in a large-scale low-speed wind-tunnel facility using the transient liquid crystals technique. They showed that major leakage flow existed in the midchord region and that the unsteady wake effect increased the Nusselt number at a large tip gap (3%), but the effect diminished with the decrease of tip gaps. Dunn and Haldeman[11] measured time-averaged heat flux at recessed blade tips for a full-scale rotating turbine stage at transonic vane exit conditions. They found that the Nusselt number on the floor of the recess near the leading edge of the blade and on the suction-side lip was in excess of the blade stagnation value.

Presented as paper 2002-3012 at the AIAA/ASME 8th Joint Thermophysics and Heat Transfer Conference, St. Louis, MO, 24–26 June 2002; received 19 August 2002; revision received 22 December 2002; accepted for publication 23 December 2002. 

*Postdoctoral Research Associate, Turbine Heat Transfer Laboratory, Department of Mechanical Engineering.

†Marcus C. Easterling Chair Professor, Turbine Heat Transfer Laboratory, Department of Mechanical Engineering. Associate Fellow AIAA.

Some researchers have carried out numerical investigations to predict blade-tip heat transfer. Ameri and Steinthorsson[12,13] predicted the heat transfer on the tip of the space shuttle main engine (SSME) rotor blade. Ameri et al.[14] computed flow and heat transfer on the tip of a GE-E$^3$ first-stage rotor blade for both smooth and recessed tips. Ameri et al.[15] also predicted the effects of tip clearance and casing recess on heat transfer and stage efficiency for several squealer blade-tip geometries. Ameri and Bunker[16] performed a computational study to investigate detailed heat-transfer distributions on blade-tip surfaces for a large power generation turbine and compared with the experimental data of Bunker et al.[7]

Rhee et al.[17] studied the local heat/mass transfer on the stationary shroud with blade-tip clearances for flat tip geometry. They used the naphthalene sublimation method and concluded that the heat/mass-transfer characteristics changed significantly with the gap clearance. Jin and Goldstein[18,19] measured local mass transfer on a simulated high-pressure turbine blade and near-tip surfaces. They used a naphthalene sublimation technique and investigated the effects of the exit Reynolds number, the tip gap clearance, and the turbulence intensity. Papa et al.[20] measured average and local mass-transfer coefficients on a squealer tip and winglet-squealer tip using the naphthalene sublimation technique. They also presented the flow visualization on the tip surface using an oil-dot technique.

Most of the studies just referenced focused on the heat-transfer coefficient on the blade-tip surface only. The present study used a hue-detection-based transient liquid crystals technique to obtain the heat-transfer coefficient on a blade-tip surface, shroud, and near-tip regions of the blade pressure and suction sides. Measurements were performed for the tip clearances of 1.0, 1.5, and 2.5% of blade span. This study provides comprehensive information about the heat-transfer coefficient on the blade-tip and the near-tip regions, where little experimental data are available in open literature.

## Experimental Setup

Figure 1 shows the schematic of the test facility. The test section consisted of a stationary blowdown facility with a five-bladed linear cascade. Compressed air stored in tanks entered a high-flow pneumatic control valve. The controller received feedback from downstream and could maintain the downstream velocity within ±3% of the desired setting value. The cascade inlet dimensions were 31.1 cm wide and 12.2 cm high. The test section's top, bottom, and sides were made of 1.27-cm-thick polycarbonate plate for the pressure measurement test. For the heat-transfer test, however, the top was replaced with a 1.27-cm-thick clear acrylic plate for best optical access to the blade tip. Two adjustable trailing-edge tailboards were used to provide identical flow conditions through the two passages adjacent to the center blade. A turbulence-generating grid of 57% porosity was placed 26.7 cm upstream of the center blade. The turbulence intensity was measured 6 cm upstream of the center blade with a TSI IFA-100 unit. In this test turbulence intensity with a turbulence-generating grid was 9.7%. The turbulence length scale was estimated to be 1.5 cm, which is slightly larger than the grid size. Figure 2 shows the definition of the blade tip and shroud. The tip

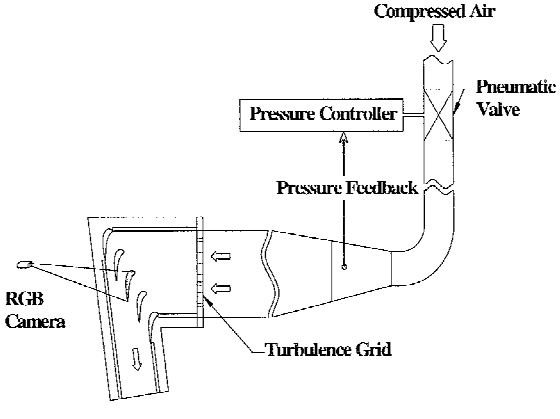


**Fig. 1 Schematic of blowdown facility.**

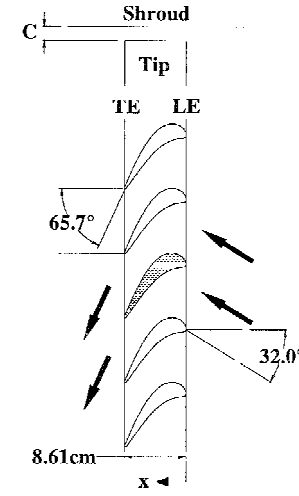


**Fig. 2 Definitions of blade tip and shroud.**

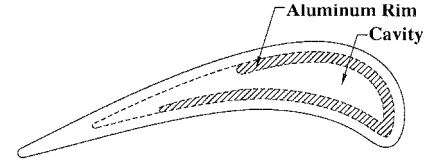


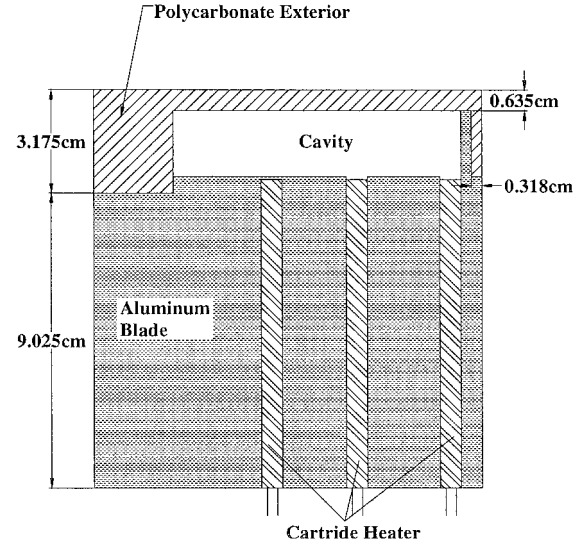


**Fig. 3 Heat-transfer measurement blade.**

gaps used for this study were 1.31, 1.97, and 3.29 mm, which correspond to about 1.0, 1.5, and 2.5% of the blade span (12.2 cm). Hard gaskets of desired thickness were placed on top of the side walls, the trailing-edge tailboard, and two outer guide blades to create tip gaps of desired height.

During the blowdown test, the inlet air velocity was set at 85 m/s and the exit velocity at 199 m/s, and the inlet and exit Mach numbers were 0.25 and 0.59, respectively. The Reynolds number based on axial chord length and exit velocity was $1.1 \times 10^6$. The inlet total pressure was 126.9 kPa, and exit static pressure was 102.7 kPa, which gave an overall pressure ratio (inlet total pressure/exit static pressure) of 1.2. Detailed flow conditions, such as the flow periodicity in cascade, are described by Azad et al.[8]

The blades were made of aluminum and finished with an EDM machine. Each blade had a 12.2 cm span and 8.61 cm axial chord length. These were three times larger than the dimension of a GE-E$^3$ blade-tip profile. Each blade had a constant cross section for the entire span. Figure 3 represents the heat-transfer measurement blade. The lower portion of the blade was made of aluminum and had three holes for cartridge heaters. The upper portion had an inner aluminum rim with a cavity and an outer shell that was made of

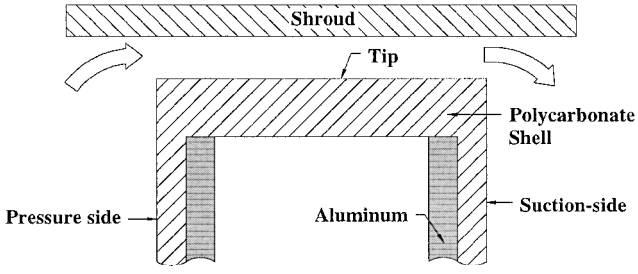


**Fig. 4 Detailed view of the blade tip.**

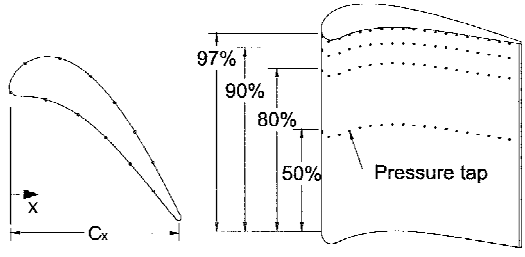


**Fig. 5a Definition of blade coordinate and location of pressure taps on the blade.**

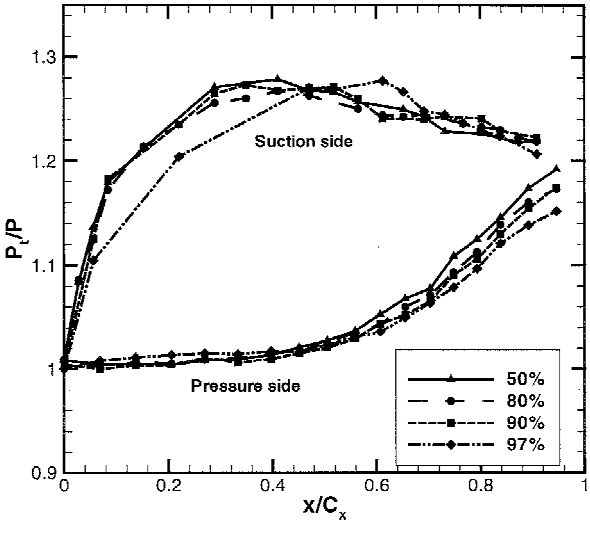


**Fig. 5b Pressure distributions on the blade pressure and suction side with $C = 1.5\%$.**

black polycarbonate with low thermal conductivity. Figure 4 shows a detailed view of the blade tip. Three cartridge heaters were inserted into the aluminum blade. The cartridge heater provided heat to the aluminum core, which heated the outer polycarbonate shell. For the heat-transfer measurement on the shroud, a 300-W plate heater was used to heat the shroud plate.

## Pressure Measurement and Results

Figure 5a shows the definition of blade coordinate and the location of pressure taps on the blade. The pressure taps were located at 50, 80, 90, and 97% height of the blade span on both the blade pressure and suction side. Figure 5b presents the ratio of the inlet total to the local static pressure along the blade at different blade span heights. The pressure was measured with 1.5% of tip gap clearance. The static-pressure difference between the pressure and suction side is the main driving force of the leakage flow. Figure 5b shows that the maximum static-pressure difference on the midspan occurred near 40% of $x/C_x$. The location of the maximum static-pressure difference has shifted toward the trailing edge at 97% of the blade span, and the maximum static-pressure difference occurs near 60% of $x/C_x$. This shift is caused by the leakage flow through the tip gap.

To investigate the pressure distribution on the shroud, 46 pressure taps were instrumented on the shroud surface. Figure 6 shows the inlet total-pressure to the local static-pressure ratio $P_t/P$ distributions on the shroud surface for the different tip gap clearances. A higher value of $P_t/P$ corresponds to a lower static pressure (high velocity), whereas a lower value corresponds to a higher static pressure (low velocity). The black curves in the contours indicate blade location under the shroud. The $P_t/P$ distribution could show the path of the leakage flow. The relatively high $P_t/P$ near $30 \sim 60\%$ of the blade chord might indicate that main leakage flow occurs in this region. As tip gap increases, $P_t/P$ increases (velocity increases), and the high $P_t/P$ region moves toward the trailing edge. The shift of the $P_t/P$ contour indicates that the path of leakage flow moves toward the trailing edge as the tip gap clearance increases.

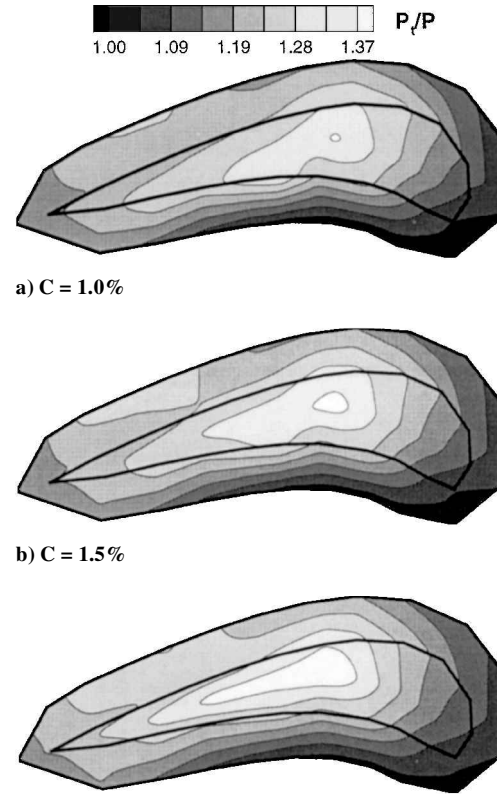


**a) C = 1.0%**

**b) C = 1.5%**

**c) C = 2.5%**

**Fig. 6 Pressure distributions on the shroud surface.**

## Heat-Transfer Measurement Theory

A hue-detection-based transient liquid crystals technique was used to measure the heat-transfer coefficient on the blade tip. The local heat-transfer coefficient over a liquid crystals coated surface can be obtained using a one-dimensional semi-infinite solid assumption for the test surface. The one-dimensional transient conduction equation, the initial condition, and the convective boundary condition are

$$k\frac{\partial^2 T}{\partial x^2} = \rho c_p \frac{\partial T}{\partial t} \tag{1}$$

at

$$t = 0, \qquad T = T_i \tag{2}$$

at

$$x = 0, \qquad -k\frac{\partial T}{\partial X} = h(T_w - T_m) \qquad \text{as } x \to \infty, \quad T = T_i \tag{3}$$

The solution to the preceding equations at the convective boundary surface ($x = 0$) is the following:

$$\frac{T_w - T_i}{T_m - I_i} = 1 - \exp\left(\frac{h^2 \alpha t}{k^2}\right) \operatorname{erfc}\left(\frac{h\sqrt{\alpha t}}{k}\right) \tag{4}$$

By knowing the initial temperature $T_i$ of the test surface, the mainstream temperature $T_m$ at the cascade inlet, and the color change

temperature $T_w$ at time $t$, the local heat-transfer coefficient $h$ can be calculated from Eq. (4). If the mainstream temperature changes with time, the varying temperature can be represented as a series of step change. Using Duhamel's superposition theorem, Eq. (4) can be written as follows:

$$T_w - T_i = (T_{m,0} - T_1) \times F\left(\frac{h\sqrt{\alpha t}}{k}\right) + \sum_{i=1}^{n}\left[F\left(\frac{h\sqrt{\alpha(t-\tau_i)}}{k}\right)\Delta T_{m,i}\right] \quad (5)$$

where

$$F(x) = 1 - \exp(x^2)\,\mathrm{erfc}(x)$$

and $\Delta T_m$ is a step change in the mainstream.

The experimental uncertainty was calculated by the methods of Kline and McClintock.[21] Note that the blade-tip material (polycarbonate) has a very low thermal conductivity of 0.18 W/mK. The liquid crystals' color change transition occurs at the surface, which is kept at a uniform initial temperature. Test duration is smaller (10–30 s) than the time required for the temperature to penetrate the full thickness of the blade-tip material. Thus, a one-dimensional transition, semi-infinite solid assumption is valid throughout the surface, except near the tip edges. The individual uncertainties in the measurement of the time of color change ($\Delta t = \pm 0.5$ s), the mainstream temperature ($\Delta T_m = \pm 0.5°C$), the color change temperature ($\Delta T_w = \pm 0.2°C$), the initial temperature ($\Delta T_i = \pm 1°C$), and the blade-tip material properties ($\Delta\alpha/k^2 = \pm 5\%$) were included in the calculation of the overall uncertainty of heat-transfer coefficient. The uncertainty for the local heat-transfer coefficient was estimated to be $\pm 8\%$. However, the uncertainty near the blade-tip edge might be much greater up to 15% as a result of the two-dimensional heat-conduction effect. The uncertainty in the high heat-transfer region also might be higher as a result of the short color change time.

## Heat-Transfer Measurement and Results

Two different liquid crystals were used in this study. The 20°C bandwidth liquid crystals (R34C20W, Hallcrest) were used to measure the initial temperature of the tip surface, and the 4°C bandwidth liquid crystals (R29C4W, Hallcrest) were used to measure the color changing time. Calibration was performed to find the hue vs temperature relation. A foil heater was placed at the bottom of a 0.635-cm-thick copper plate. The black paint (BB-G1, Hallcrest) and liquid crystals were sprayed on the copper plate. Input voltage to the heater was set properly in order to increase the surface temperature by 0.6°C, and enough time was allowed for the temperature to be steady at each temperature step. The surface temperature was then read by a thermocouple that was attached at the surface of the copper plate, and the color of the liquid crystals was recorded to the computer. At each temperature step the hue was calculated from the stored image, and the relation between hue and temperature was established for both 20°C and 4°C bandwidth liquid crystals. Figure 7a shows the results of the calibration for both liquid crystals.

Before the transient test the black paint and 20°C bandwidth liquid crystals were sprayed uniformly on the test surface, and the test surface was heated. After the surface temperature reached the desired temperature (about 70°C), the color of the liquid crystals on the test surface was recorded by a RGB color charge-coupled device (CCD) camera with 24-bit color frame grabber board. From every pixel of the stored image, hue was calculated, and the initial temperature of the test surface was determined using the precalibrated hue vs temperature relation. Figure 7b presents the initial temperature on the tip for $C = 1.5\%$ case.

After the initial temperature measurement on the blade tip, the 20°C bandwidth liquid crystals were removed, and the black paint and the 4°C bandwidth liquid crystals were sprayed on. The blade tip was heated until the reference temperatures became the same as those of the initial temperature measurement test. Reference temperatures were measured by thermocouples located inside the cavity

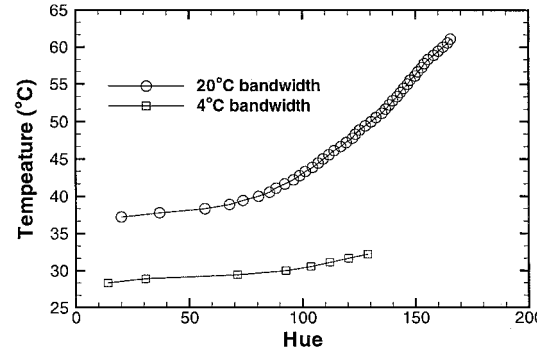


**Fig. 7a Relation between hue and temperature.**

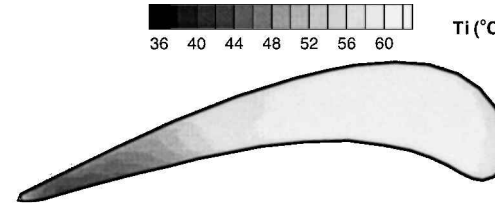


**Fig. 7b Initial temperature on the tip for $C = 1.5\%$.**

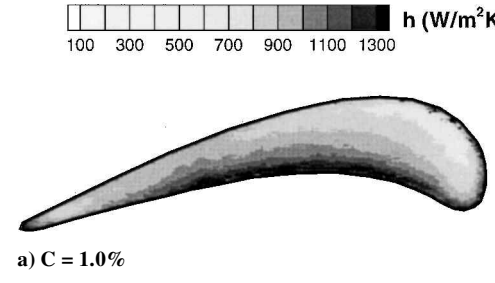


**a) C = 1.0%**

**b) C = 1.5%**

**c) C = 2.5%**

**Fig. 8 Heat-transfer coefficient on the blade tip.**

and the shroud surface to ensure the same temperature conditions for the initial temperature measurement and the transient tests. After temperatures reached the desired value, the compressed air was allowed to flow by turning on the flow controller. When the mainstream velocity reached the preset value, the color change of the liquid crystals was recorded at the speed of 30 frames per second. The test duration time was short enough (10–30 s) to make a semi-infinite solid assumption. From every pixel at each stored image, hue was evaluated and used to calculate the time from the initial condition (about 40–60°C, depending on location) to a given hue value (50), which corresponded to the temperature of 29°C for the tip and shroud test, and 29.6°C for the pressure and suction sides test. Then, the heat-transfer coefficient $h$ was calculated from Eq. (5).

### Heat-Transfer Coefficient on the Blade Tip

Figure 8 shows the heat-transfer coefficient distributions on the blade tip. All cases show high heat-transfer coefficients near the pressure side of 20 ~ 70% of the blade chord. This high heat-transfer

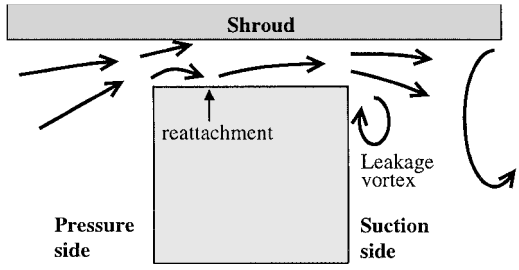


**Fig. 9 Conceptual view of flow near blade tip.**

region corresponds to the maximum leakage flow region caused by the large pressure difference between the blade pressure and suction sides as shown in Fig. 6. The high heat-transfer region exists near the pressure side edge, and the heat-transfer coefficient on that region gradually decreases towards the suction side. A low heat-transfer coefficient exists along the pressure side tip. Those trends are caused by the flow separation and reattachment on the tip surface, as shown in Fig. 9. Figure 9 illustrates the conceptual view of the flow near the blade tip. As the flow tries to leak through the tip gap, the flow separates and reattaches on the tip surface and causes the low and high heat-transfer coefficients near the pressure side edge. On the suction side of the blade, the interaction between the leakage flow and passage vortex can create the leakage vortex. There is a low heat-transfer region near the suction side of the leading edge, and this trend corresponds with Bunker et al.[7] and Azad et al.[8] The range of heat-transfer coefficient is from about 600 to 1300 W/m$^2$K.

As the tip gap clearance increases, the heat-transfer coefficient generally increases except very near the pressure side edge. As the tip gap clearance increases, the size of the separation region (low heat-transfer coefficient region) very near the pressure side edge also increases. And the high heat-transfer region near 20 ~ 70% of the blade chord moves toward the trailing-edge side as the tip gap clearance increases. That might be caused by the change of the path of the leakage flow, as shown in Fig. 6. As the tip gap clearance increases, the path of leakage flow can move toward the trailing edge side and result in a larger low heat-transfer region near the suction side of the leading edge.

### Heat-Transfer Coefficient on the Shroud

Figure 10 shows the heat-transfer coefficient distribution on the shroud surface. All tip gap clearance cases show maximum heat-transfer regions near 20 ~ 70% of the blade chord and low heat-transfer regions near the leading edge. These trends correspond with the pressure results (Fig. 6) and the blade-tip results (Fig. 8).

A relatively higher heat-transfer region exists near the pressure side edge. This might be caused by the impingement of the separated leakage flow, as shown in Fig. 9. As the mainstream flow tries to leak through the tip gap, the flow separates from the blade-tip surface, and the separation region can be seen near the pressure side edge, as shown in Fig. 9. After flow separates from the tip surface, the flow can impinge on the shroud surface and result in a high heat-transfer region above the pressure side edge.

Downstream of the blade suction side, a relatively high heat-transfer region exists. This region might result from the interaction between the leakage vortex and the mainstream flow. The highest shroud heat-transfer coefficient is about 800 W/m$^2$K, and this is about 65% of that on the blade tip. The lowest heat-transfer coefficient on the shroud can be seen on the pressure side as a result of low velocity along the pressure side of the blade (see Fig. 6).

As the tip gap clearance increases, the high heat-transfer region downstream of the suction side expands to farther downstream. This trend corresponds with Rhee et al.[17]

### Heat-Transfer Coefficient on the Near Tip of the Pressure Side

Figure 11 shows the heat-transfer-coefficient distribution on the near-tip region of the pressure side. The height of the test area was 2.5 cm from the blade tip, which corresponds to about 20% of the blade span. Results show high heat-transfer coefficients near the

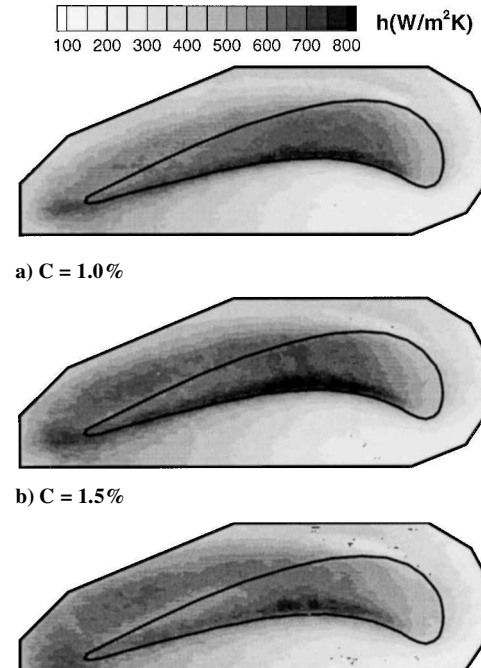


**Fig. 10 Heat-transfer coefficient on the shroud.**

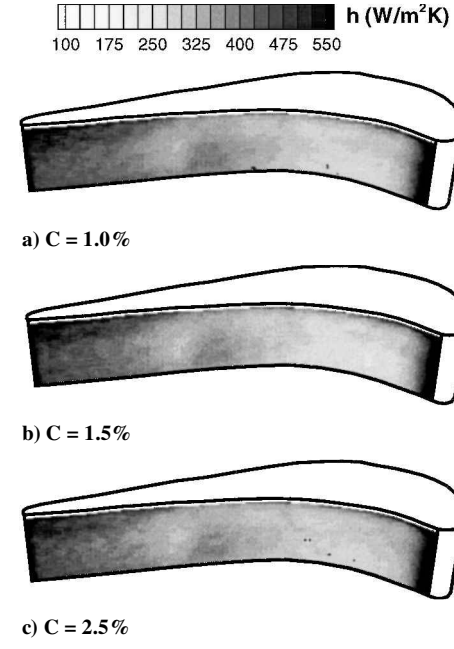


**Fig. 11 Heat-transfer coefficient on the pressure side.**

leading and trailing edges. The distribution of the heat-transfer coefficient is almost two-dimensional along the blade span except at very near the pressure side tip. The entrance effect on the leakage flow increases the heat-transfer coefficient on the near-tip region, as shown in Fig. 9. The highest value of the pressure side heat-transfer coefficient is about 550 W/m$^2$K and is about 45% of that on the blade tip. This is because the velocity along the pressure side is much lower than along the suction side of the blade, as shown in Fig. 6. The effect of the tip gap clearance on the pressure side heat transfer seems to be negligible. The trend and value of the pressure side heat-transfer coefficient is almost the same for all tip gap clearances.

### Heat-Transfer Coefficient on the Near Tip of the Suction Side

Figure 12 shows the heat-transfer-coefficient distribution on the near-tip region of the suction side. The height of the test area was

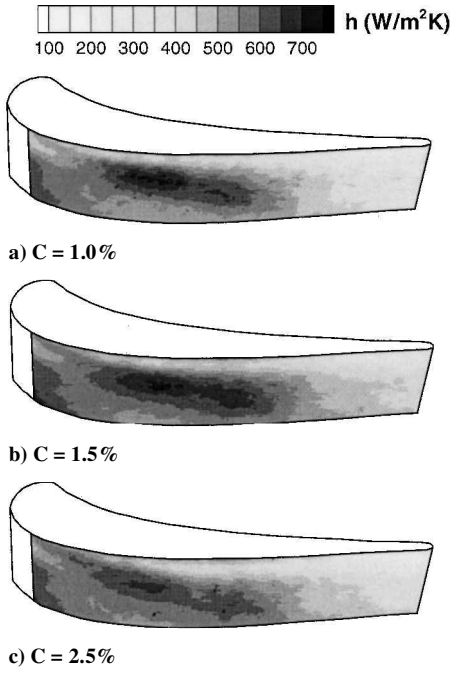


**Fig. 12 Heat-transfer coefficient on the suction side.**

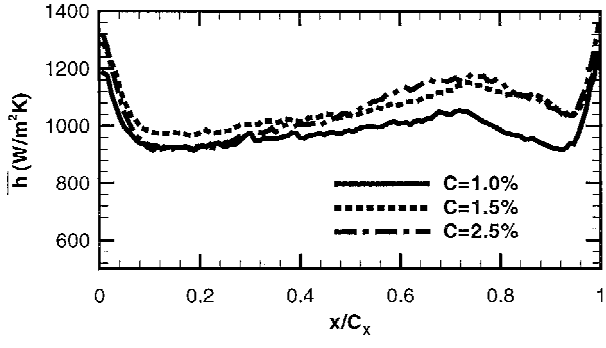


**Fig. 13 Averaged heat-transfer coefficient on the blade tip.**

2.5 cm from the blade tip, which corresponds to about 20% of the blade span. Because of the large view angle between the camera and the test surface, data could not be taken from the region close to the leading edge. The range of the heat-transfer coefficient is from about 300 to 700 W/m$^2$K. The peak value of the suction side heat-transfer coefficient is about 55% of that on the blade tip. The high heat-transfer region starts from about 30% of the blade chord. This region corresponds with the beginning region of the leakage flow exiting from the tip gap, as shown in Fig. 6. As the leakage flow exits to the suction side, the leakage vortex and the interaction between the leakage vortex and the mainstream can result in a high heat-transfer region along the suction side.

The heat-transfer coefficient on the suction side is not affected much by the tip gap clearance. The trend and value of the suction-side heat-transfer coefficient is almost the same for all tip gap clearances.

### Averaged Heat-Transfer Coefficient

Figures 13–16 show the averaged heat-transfer coefficient on the tip, shroud, and near-tip regions of the pressure and suction sides, respectively. The local heat-transfer coefficients are averaged at a given $x/C_x$ location. For the shroud the average was taken from the region above the tip only. Results show that the heat-transfer coefficient on the tip (Fig. 13) increases as tip gap clearance increases. The heat-transfer coefficients on the shroud above the tip (Fig. 14) and on the suction side (Fig. 16) increase and then decrease as the tip gap clearance increases. The heat-transfer coefficient on the pressure side (Fig. 15) is insensitive to the tip gap clearance. The heat-transfer coefficient on the pressure side shows similar trend and value.

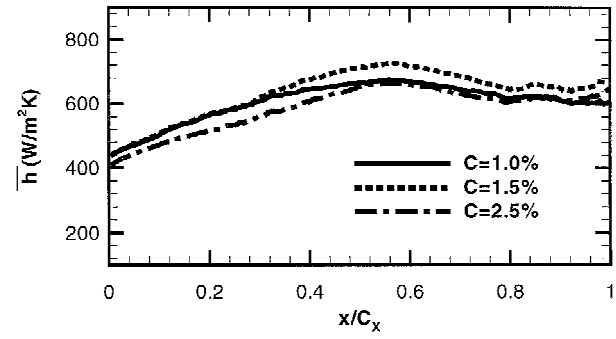


**Fig. 14 Averaged heat-transfer coefficient on the shroud.**

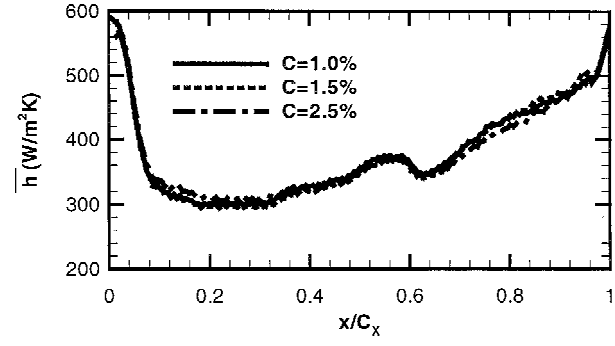


**Fig. 15 Averaged heat-transfer coefficient on the pressure side.**

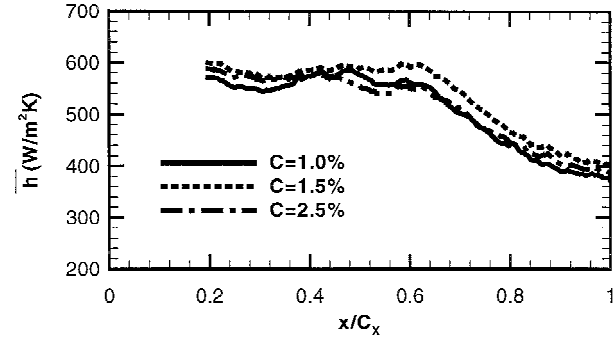


**Fig. 16 Averaged heat-transfer coefficient on the suction side.**

## Conclusions

The major findings based on the experimental results are as follows:

1) Pressure and heat-transfer coefficient measurements showed that the heat-transfer-coefficient distribution on the tip and the shroud surface were similar and corresponded with the leakage flow path through the tip gap clearance.

2) The highest heat-transfer coefficient (about 1250 W/m$^2$K) was found near the pressure side of the blade tip, where the leakage flow separated and then reattached on the tip surface. The heat-transfer coefficient was smaller near the suction side of the tip caused by leakage flow development. The low heat-transfer region caused by the separation of the leakage flow existed near the pressure side edge of the tip.

3) The higher heat-transfer coefficient existed on the shroud above the pressure side edge of the tip caused by the impingement of the separated leakage flow. The peak heat-transfer coefficient on the shroud was about 65% of that on the tip surface.

4) The heat-transfer coefficient on the near-tip region of the blade pressure side showed a two-dimensional distribution except at very near the pressure side tip, and the overall value was less than 45% of that on the tip.

5) The heat-transfer coefficient on the near-tip region of the blade suction side showed the possible trace of the leakage vortex on the

suction side. The peak value of the heat-transfer coefficient was about 55% of that on the tip.

6) In general, the heat-transfer coefficient on the tip was higher than that on the shroud and near-tip region of the suction side of the blade. The heat-transfer coefficient on the near-tip region of the blade pressure side was the lowest.

7) As tip gap clearance increased, in general, the heat-transfer coefficient on the tip surface increased. The heat-transfer coefficient on the near-tip region of the blade pressure side was insensitive to the tip gap clearance. However, the effect of the tip gap clearance on the heat-transfer coefficient on the shroud and near-tip region of the blade suction side did not show a consistent trend.

## Acknowledgments

This work was prepared with the support of the NASA Glenn Research Center under Grant Number NAG3-2002. The NASA technical team is Robert Boyle and Raymond Gaugler. Their support is greatly appreciated. Technical discussions with C. Pang Lee of General Electric Aircraft Engines, Ron Bunker of General Electric R&D Center, and GM S. Azad of Siemens-Westinghouse were helpful and are acknowledged.

## References

[1]Mayle, R. E., and Metzger, D. E., Heat Transfer at the Tip of an Unshrouded Turbine Blade," *Proceedings of the Seventh International Heat Transfer Conference*, Vol. 3, Hemisphere, New York, 1987, pp. 87–92.

[2]Metzger, D. E., and Rued, K., "The Influence of Turbine Clearance Gap Leakage on Passage Velocity and Heat Transfer Near Blade Tips. Part I: Sink Flow Effects on Blade Pressure Side," *Journal of Turbomachinery*, Vol. 111, No. 3, 1989, pp. 284–292.

[3]Rued, K., and Metzger, D. E., "The Influence of Turbine Clearance Gap Leakage on Passage Velocity and Heat Transfer Near Blade Tips. Part II: Source Flow Effects on Blade Pressure Side," *Journal of Turbomachinery*, Vol. 111, No. 3, 1989, pp. 293–300.

[4]Metzger, D. E., Bunker, R. S., and Chyu, M. K., "Cavity Heat Transfer on a Transverse Grooved Wall in a Narrow Flow Channel," *Journal of Heat Transfer*, Vol. 111, No. 1, 1989, pp. 73–79.

[5]Chyu, M. K., Moon, H. K., and Metzger, D. E., "Heat Transfer in the Tip Region of Grooved Turbine Blades," *Journal of Turbomachinery*, Vol. 111, No. 2, 1989, pp. 131–138.

[6]Metzger, D. E., Dunn, M. G., and Hah, C., "Turbine Tip and Shroud Heat Transfer," *Journal of Turbomachinery*, Vol. 113, No. 3, 1991, pp. 502–507.

[7]Bunker, R. S., Baily, J. C., and Ameri, A. A., "Heat Transfer and Flow on the First Stage Blade Tip of a Power Generation Gas Turbine: Part 1: Experimental Results," *Journal of Turbomachinery*, Vol. 122, No. 2, 2000, pp. 272–277.

[8]Azad, G. M. S., Han, J. C., Teng, S., and Boyle, R., "Heat Transfer and Pressure Distributions on a Gas Turbine Blade Tip," *Journal of Turbomachinery*, Vol. 122, No. 4, 2000, pp. 717–724.

[9]Azad, G. M. S., Han, J. C., and Boyle, R., "Heat Transfer and Pressure Distributions on the Squealer Tip of a Gas Turbine Blade," *Journal of Turbomachinery*, Vol. 122, No. 4, 2000, pp. 725–732.

[10]Teng, S., Han, J. C., and Azad, G. M. S., "Derailed Heat Transfer Coefficient Distributions on a Large-Scale Gas Turbine Blade Tip," *Journal of Heat Transfer*, Vol. 123, No. 4, 2001, pp. 803–809.

[11]Dunn, M. G., and Haldeman, C. W., "Time-Averaged Heat Flux for a Recessed Tip, Lip, and Platform of a Transonic Turbine Blade," *Journal of Turbomachinery*, Vol. 122, No. 4, 2000, pp. 692–697.

[12]Ameri, A. A., and Steinthorsson, E., "Prediction of Unshrouded Rotor Blade Tip Heat Transfer," American Society of Mechanical Engineers, Paper 95-GT-142, June 1995.

[13]Ameri, A. A., and Steinthorsson, E., "Analysis of Gas Turbine Rotor Blade Tip and Shroud Heat Transfer," American Society of Mechanical Engineers, Paper 96-GT-189, June 1996.

[14]Ameri, A. A., Steinthorsson, E., and Rigby, L., David, "Effect of Squealer Tip on Rotor Heat Transfer and Efficiency," *Journal of Turbomachinery*, Vol. 120, No. 4, 1998, pp. 753–759.

[15]Ameri, A. A., Steinthorsson, E., and Rigby, L., David, "Effects of Tip Clearance and Casing Recess on Heat Transfer and Stage Efficiency in Axial Turbines," *Journal of Turbomachinery*, Vol. 121, No. 4, 1999, pp. 683–693.

[16]Ameri, A. A., and Bunker, R. S., "Heat Transfer and Flow on the First Stage Blade Tip of a Power Generation Gas Turbine: Part 2: Simulation Results," *Journal of Turbomachinery*, Vol. 122, No. 2, 2000, pp. 272–277.

[17]Rhee, D. H., Choi, J. H., and Cho, H. H., "Effect of Blade Tip Clearance on Turbine Shroud Heat/Mass Transfer," American Society of Mechanical Engineers, Paper 2001-GT-0158, June 2001.

[18]Jin, P., and Goldstein, R. J., "Local Mass/Heat Transfer on a Turbine Blade Tip," The 8th International Symposium on Transport Phenomena and Dynamics of Rotating Machinery, Vol. 1, Pacific Center of Thermal-Fluids Engineering, Honolulu, Hawaii, 2000, pp. 556–563.

[19]Jin, P., and Goldstein, R. J., "Local Mass/Heat Transfer on Turbine Blade Near-Tip Surfaces," American Society of Mechanical Engineers, Paper GT-2002-30556, June 2002.

[20]Papa, M., Goldstein, R. J., and Gori, F., "Effects of Tip Geometry and Tip Clearance on the Mass/Heat Transfer from a Large-Scale Gas Turbine Blade," American Society of Mechanical Engineers, Paper GT-2002-30192, June 2002.

[21]Kline, S. J., and McClintock, F. A., "Describing Uncertainties in Single Sample Experiments" *Mechanical Engineering*, Vol. 75, No. 1, 1953, pp. 3–8.